Available online at www.CivileJournal.org

Civil Engineering Journal

(E-ISSN: 2476-3055; ISSN: 2676-6957)

Vol. 11, No. 11, November, 2025

Shear Strength of One-Way Slabs Subjected to Concentrated Loads

Ahmed F. Al-Bayati [1*], Omar S. Farhan [2], Zahir Noori M. Taki [1]

[1] Department of Civil Engineering, College of Engineering, Al-Nahrain University, 64040 Baghdad, Iraq.

[2] Department of Architectural Engineering, Al-Nahrain University, 64040 Baghdad, Iraq.

Received 03 February 2025; Revised 17 September 2025; Accepted 27 September 2025; Published 01 November 2025

Abstract

Reinforced concrete (RC) one-way slabs without transverse reinforcement are found extensively in bridge constructions. In the presence of concentrated loads (CLs) close to the supports, the shear strength (SS) of such slabs is usually determined using design expressions provided by the codes of practice that were derived originally from tests performed on beams or one-way slabs that were loaded along their entire width, which are inconsistent with the actual shear failure mechanism of one-way slabs under CLs. This paper presents an empirical SS model developed using the gene expression programming method (GEP), where the SS is related to six influencing parameters. The proposed model is derived employing the test results of 238 RC one-way slabs that experienced shear failure from the literature. The accuracy of the proposed model is measured using several statistical indices and compared with the existing shear design methods. The GEP model agreed favorably with the test results. The GEP model was also employed to conduct a parametric study for further validation and sensitivity analysis to define the contribution of input parameters to the SS. The parametric study demonstrated the efficiency of the GEP model in replicating the physical behavior, and the sensitivity analysis revealed that the SS is sensitive to the concrete strength and the shear span-effective depth ratio.

Keywords: Bridge, One-Way Slabs; Shear Design; Concentrated Loads; Gene Expression Programming.

1. Introduction

Reinforced concrete (RC) one-way slabs are structural members that transfer loads in one direction perpendicular to the supports. They are subject to closely spaced, highly concentrated vehicle loads near supports in bridge constructions. Examples of these are slab bridges, deck slabs supported on girder bridges, and box-girder bridges [1], as shown in Figure 1. Because of the loading situation, such slabs are susceptible to shear failure characterized by diagonal cracks extending from the concentrated loads (CLs) to the supports [1-3]. Despite the increase in traffic volume and the brittle nature of shear failure, only a few studies were conducted to investigate the shear mechanism of one-way slabs under CLs [4]. Consequently, their shear design procedure has not been addressed in the provisions of the design codes [1, 2, 5, 6].

The codes of practice provide semi-empirical methods [7-9] and mechanical methods [10, 11] to design RC slabs against one-way and two-way shear. The one-way shear equations were derived using shear tests conducted on heavily reinforced slender beams, while those of two-way shear were derived using punching shear (PS) tests on slab-column connections [12]. The applicability of these methods is questionable since the shear transfer mechanism of one-way slabs under CLs is different from those of ordinary beams and slab-column connections (see Figure 2), as it is considered an intermediate case between them [13]. The results of previous experimental and analytical investigations reflect these differences and confirm that they affect the slabs' shear strength (SS) [1, 3].

* Corresponding author: ahmed.f.al-bayati@nahrainuniv.edu.iq

http://dx.doi.org/10.28991/CEJ-2025-011-11-013

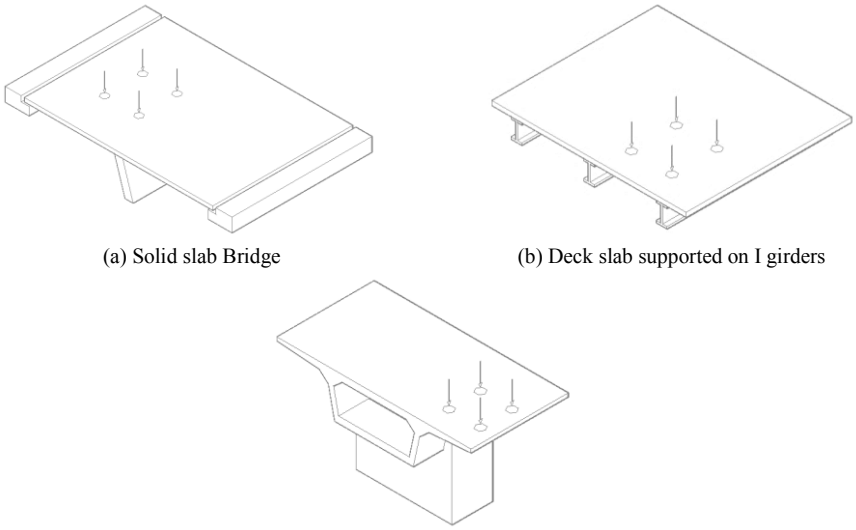

(a) Solid slab Bridge (b) Deck slab supported on I girders

(c) Box girder

Figure 1. Examples of RC slabs one-way under CLs

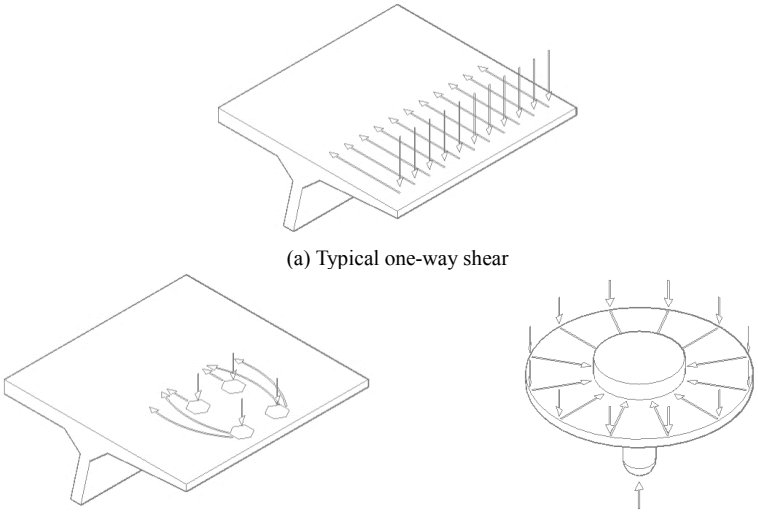

(a) Typical one-way shear

(b) One-way slab under CLs (c) Typical two-way shear

Figure 2. Shear transfer mechanism in RC slabs

Researchers found that the SS of one-way slabs without shear reinforcements is significantly affected by several parameters, such as the concrete strength, the shear span-effective depth ratio, the size of CLs, and the slab's width. The SS increases with the size of CLs and the slab's width to a certain limit [3, 14-16] and decreases with the increase in the shear span-effective depth ratio [1-3]. They also found that the amount of transverse reinforcement, the type of steel rebars (plain or deformed), and the moment-shear ratio of the section have little to do with the SS [3, 12, 17], while some researchers indicated that the degree of rotational restraint has an ambiguous effect on the SS [3].

Few design models are available to predict the shear capacity of RC one-way slabs under CLs, where these models constitute a refinement of Eurocode 2 for one-way shear [6, 18]. Lantsoght et al. [19] have suggested a strip model based on the plasticity approach. The drawback of this model is that the shear calculations require adjustment to fit the geometry of the deck under consideration [20]. Abambres & Lantsoght [20] employed the artificial neural network (ANN) approach to predict the SS of one-way slabs under CLs, which perfectly matched the test results. The shear calculations, however, are carried out using non-accessible matrices.

Kongwang et al. [21] proposed a fatigue shear degradation model for RC deck slabs under wheel loads. Their model included the SS and S-N equations, considering the influence of environmental and support parameters, where a beam-like structure is employed to predict the fatigue life of a deck slab under wheel loads. Fernández et al. [22] proposed an SS model considering the effects of the concrete strength, the size of a slab, and the shear span-effective depth ratio. They employed the EC2 [8] French method in defining bw. However, they considered the angle to be 52.5 degrees instead of 45 degrees, as the average value of α as suggested by the Model Code [10], for simplicity to be valid for RC slabs with different restraint conditions. They verified their model with 90 slabs from the literature. Huber et al. [23]

reported the results of four shear tests conducted on two full-scale models of bridge slabs constructed with bent-up bars and subject to CLs simulating the EC2 train loads. The current design codes were applied to predict the SS of the existing bridge slabs. The comparisons with the test results revealed that the ACI-318-25 [7], EC2 [8], and Model Code [10] underestimated the SS of the slabs constructed with bent-up bars due to detailing issues. Lipari [24] carried out a numerical analysis to investigate the shear behavior of design skew slab bridges without shear reinforcement under CLs. The results indicated that the shear behavior is generally similar to ordinary slabs despite the stress concentrations at the obtuse corners. Lipari compared the numerical results with the shear current design codes and found that the EC2 [8] and the Model Code [10] underestimated the SS and provided scattered predictions. Setiawan et al. [25] performed numerical analysis to study the shear failure of cantilever bridge deck slabs subjected to CLs, where the internal forces were evaluated considering the gradual reduction in shear stiffness in terms of bending moment and shear forces. They found that the failure mechanism is similar to the shear in beams without transverse reinforcement instead of PS, and the reduction in shear stiffness is significant near the support because of the high bending moment causing high shear strain because of the formation of inclined flexural cracks.

The previous models have provided better strength predictions than existing models. However, some of them either do not consider the governing parameters, or they were calibrated with a small database, and consequently, they provide scattered strength estimations. Hence, there is a need to develop a reliable design method considering all the key parameters and verifying using a comprehensive database. Recently, gene expression programming (GEP) has proved to be an efficient approach in various civil engineering applications, as evidenced by experimental results [26-28]. The GEP overpasses regression analysis since it does not need a predetermined function, and it can develop an explicit expression by including and excluding input parameters to achieve the best fitness with the test results.

This paper presents a predictive model for the SS of one-way slabs under CLs. The proposed model is developed based on the GEP technique using the test results of 238 one-way slabs under CLs compiled from the literature. The performance of the proposed model is compared with those of the design codes for verification. This work differs from the previous studies in terms of the adopted parameters, the evolutionary approach, and the parametric and sensitivity analysis performed to develop the proposed model with consistent predictive capability using a comprehensive database. Figure 3 summarizes the workflow of this study.

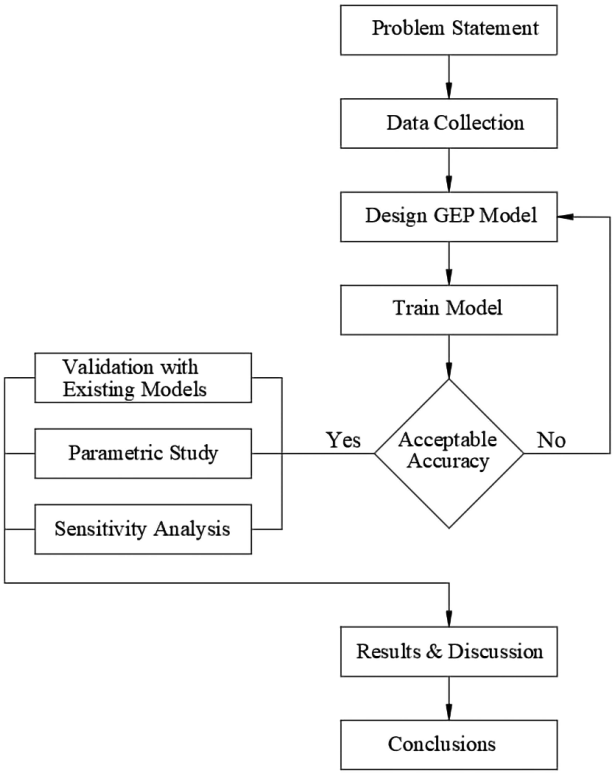

Figure 3. Research workflow

2. Slabs Database

An experimental database consisting of 238 RC one-way slabs subjected to CLs that experienced shear failure is employed to train and test the proposed GEP model. The database includes the test results of 21.6, 23, and 22 RC slabs reported by Lantsoght et al. [1], Natário et al. [2], Reissen et al. 2018 [3], and Lantsoght et al. [13], respectively; and the test results of 166 slabs reported by various researchers [13, 29-52] that were previously collected by Lantsoght et al.

[53]. The slabs employed in this study have no shear reinforcement and are either simple span, cantilever, or continuous. That is, 168 (70%) of them are simple span slabs, 52 (22%) are continuous slabs, and 18 (8%) are cantilever slabs.

According to previous experimental studies, the SS is affected by specific parameters. These include the concrete strength (f_c), the longitudinal reinforcement ratio (ρ), the ratio of the shear span to the slab's effective depth in the longitudinal direction (a/d), the slab's effective depth in the longitudinal direction (d), the slab's width (b), the ratio of the slab's width to the CL's width (b/b_l), and the ratio of the slabs' width to the slabs' effective depth in the longitudinal direction (b/d). The key parameters are employed to develop the proposed model. Table 1 presents the descriptive statistical parameters of the considered variables, such as the average value (AVG), the standard deviation (SD), the minimum value (Min), the maximum value (Max), and the range.

Table 1. Statistical details of the input parameters

Variables and data sets	Statistical parameters				
	Mean	Standard deviation	Minimum	Maximum	Range
b (mm)					
Training set	1606	1206	400	10000	9600
Testing set	1468	1136	500	3500	3000
d (mm)					
Training set	196	100	80	538	458
Testing set	233	137	81	750	669
a/d					
Training set	3.3	1.7	0.7	9.1	8.4
Testing set	3.9	0.9	1.0	5.5	4.5
f_c (MPa)					
Training set	41.8	21.0	12.7	94.8	82.1
Testing set	34.1	11.1	12.4	60.0	47.6
ρ (%)					
Training set	1.2	0.5	0.4	2.8	2.3
Testing set	1.2	0.5	0.4	2.2	1.8
b/b_l					
Training set	13.0	13.1	2.5	75.0	72.5
Testing set	7.7	3.2	1.3	20.0	18.8
b/d					
Training set	9.9	7.7	1.9	45.5	43.6
Testing set	7.1	4.7	1.3	14.6	13.3
V_{test} (kN)					
Training set	510.7	445.9	52.5	1717.0	1664.5
Testing set	387.9	304.0	59.0	1283.0	1224.0

The dataset includes a wide range of test variables, which significantly influence the SS. However, a critical review of Tables A1 and A2 in Appendix I indicates that only 30% of the slabs were tested with a/d smaller than 2.5, which interests bridge engineers. In addition, the database includes no skew slabs, and all are rectangular ones [20] because no test results of skew slabs failed by shear were found in the literature. Therefore, there is a need to carry out extensive tests to examine the influence of the above parameters on the SS.

The experimental database is split into two statistically comparable sets to train and test the proposed model. That is, 167 (70%) of the test slabs are employed for training, and the remaining 71 (30%) slabs are used for testing. The training set is to develop the relationship between the input parameters to derive the proposed model. While the testing set (remaining slabs) is to provide a neutral assessment of the proposed model. It is noteworthy that the excessive values of the considered parameters are included in the training set to allow for the fact that the GEP (empirical) model is better in interpolation than extrapolation [54].

3. Existing Models

This section summarizes four shear design expressions for one-way slabs without shear reinforcement (ACI-318-25 [7], EC2 [8], AASHTO 2007 [9], and the Model Code [10]) and the crack sliding theory (CST). The symbols used in the existing equations are unified in Table 2 for convenience, even though they are variants from the original documents. In which f_c is the cylinder compressive strength, d is the slab's effective depth in the longitudinal direction, ρ is the tension reinforcement ratio in the slab's longitudinal direction, b_w is the effective width of a slab, and av is the clear shear span. The ACI-318-25 [7], the AASHTO 2007 [9], and the CST [11] define b_w as the total width of a slab. The EC2 [8] defines b_w according to (French and Dutch methods) for wide members experiencing shear, see Figures 4-b and 4-c, while Figure 4-d shows the b_w of the Model Code [10]. All the parameters are in SI units. It is noteworthy to mention that the strength reduction and partial safety factors are set to one when compared with test results. The simplified expression of the CST [11] and the approximate method I of the Model Code [10] are considered because the information on the size of aggregates is not available for all test slabs, despite that the accuracy and the complexity of these methods increase by the use of aggregate interlock and longitudinal strain in the calculations of the SS.

Table 2. The existing SS equations

Design code	Shear equation
ACI-318-25 [7]	When $A_s \geq A_{smin}$, $V_{ACI} = \begin{bmatrix} [0.17\lambda\sqrt{f_c}]b_w d \text{ (a)} \\ [0.66\lambda\rho^{\frac{1}{3}}\sqrt{f_c}]\, b_w d \text{ (b)} \end{bmatrix}$ When $A_s < A_{smin}$ $V_{ACI} = [0.66\lambda_s\lambda\rho^{\frac{1}{3}}\sqrt{f_c}]\, b_w d$ $\lambda = 1$ for normal concrete, and $\lambda = 0.75$ for lightweight concrete. $\lambda_s = \sqrt{\frac{2}{1+0.004d}} \leq 1$, where d in mm and f_c in MPa and $\sqrt{f_c} \leq 8.3$ MPa. $V_{ACI} \leq 0.42\lambda\sqrt{f_c}b_w d$
EC2 [8]	$V_{EC2} = [0.18k(\rho f_c)^{\frac{1}{3}}]\, b_w d$ $k = 1 + \sqrt{\frac{200}{d}} \leq 2$, where d in mm and f_c in MPa. $\beta = \begin{bmatrix} 1 & if\ a_v \geq 2d \\ a_v/_{2d} & if\ 0.5d \leq a_v \leq 2d \\ 0.25 & if a_v \leq 0.5d \end{bmatrix}$ b_w and a_v as defined in Figures. 4(b)- (c) for French and Dutch practice.
AASHTO [9]	$V_{AASHTO} = [0.0525\sqrt{f_c}]b_w d + V_d + V_i \frac{M_{cre}}{M_{max}}$, where d in mm and f_c in MPa. V_d: Shear force due to dead load. V_i:Max. shear force at the section. M_{max}: Max. moment at the section. M_{cre}: Cracking moment.
Model Code 2010 [10]	$V_{MC} = [k_v\sqrt{f_c}]b_w z$, where z in mm and f_c in MPa. $k_v = \frac{180}{1000+1.25z}$, (Level approximation I) $z = 0.9d$ $\beta = \begin{bmatrix} 1 & if\ a_v \geq 2d \\ a_v/_{2d} & if\ 0.25d \leq a_v \leq 2d \\ 0.5 & if a_v \leq d \end{bmatrix}$ b_w and a_v as defined in Figure 4(d).
CSCT [11]	$V_{CSCT} = [(\frac{0.2}{1+0.0022d})\sqrt{f_c}]\, b_w d$ (simplified expression)

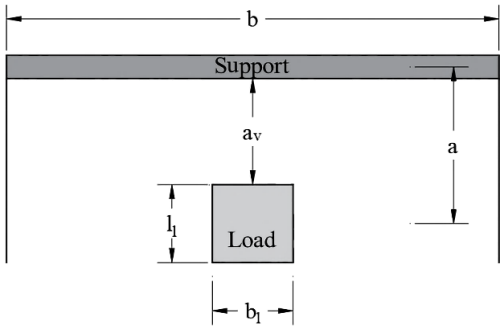

(a) Geometrical properties of a slab

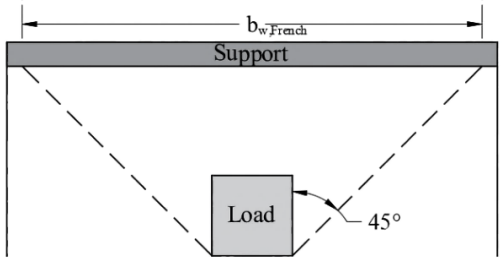

(b) Effective width of a French approach

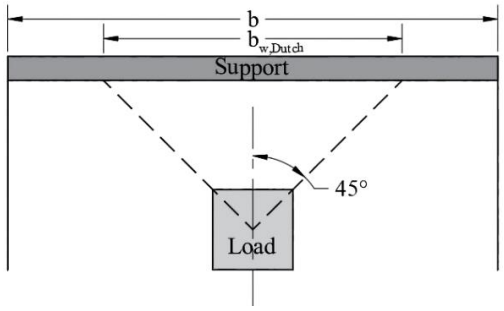

(c) Effective width of a Dutch approach

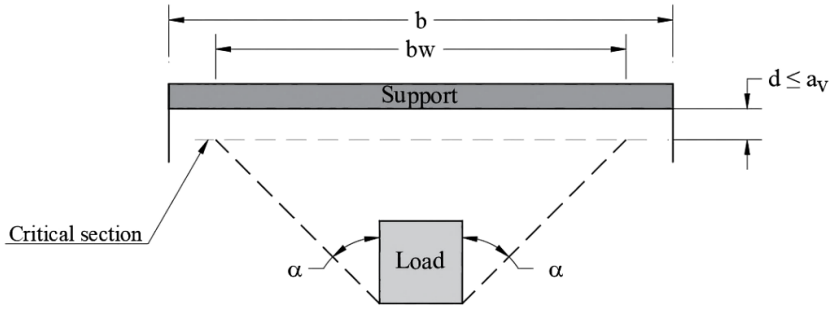

$\alpha = 45^{o}$ for clamped slabs
$\alpha = 60^{o}$ for simply supported slabs

(d) Effective width of Model code 2010

Figure 4. Geometrical properties and effective width in French and Dutch approaches

4. Gene Expression Programming

4.1. Overview

The genetic algorithm is a heuristic algorithm used to solve constrained and unconstrained optimization problems based on the Theory of Evolution [48]. The solution process starts by randomly selecting individuals according to their fitness to parent the individuals of the next generation. This process is repeated for sequential generations and stops only when the individuals have evolved to the anticipated fitness. Koza (1992) [55] developed a computer technique called genetic programming (GP) to solve particular problems. It is considered an extended form of GA, and it encodes individuals in a way different from that of GA. GP uses expression trees (ETs) of various sizes and forms, while GA uses a linear fixed-length string.

Ferreira (2002) [56] presented a technique, more advanced than GP and GA, called Gene expression programming (GEP). This technique can solve complex problems with a smaller population. In this technique, the individuals are encoded as fixed-length linear strings and described nonlinearly in ETs. Chromosomes and ETs are the keystones in building GEP models. A chromosome consists of a head and tail and usually includes gene(s) defining a mathematical formulation. The head contains constants, variables, and mathematical operators, while the tail contains terminals (constants and variables). Mathematical operators (addition, subtraction, multiplication, and division) are used to connect each gene with all.

The building of a new GEP model begins with setting fitness functions, followed by the selection of the components of the tail and head to develop the chromosomes. The number of genes and the length of the head are set to shape the architecture of the chromosomes. Finally, the linking function and mathematical operators are selected to achieve the best performance.

4.2. Development of the GEP Model

Various trials were conducted to select the optimum model that agrees best with the experimental results, and the proposed GEP model is the one that achieves the best performance. In each trial, the number of genes, the linking functions, the chromosomes, and the size of the head are varied to improve the accuracy and consistency of the proposed model. It is worth noting that the increase in the number of genes does not always increase accuracy and may induce over-fitting. In addition, an increase in the number of chromosomes may result in remarkable growth in the processing time [26, 27].

The genetic parameters determine the accuracy and generality of the GEP model. Hence, various trials were conducted to improve the accuracy and consistency of the model, where the values of these parameters were selected in each trial either from trial and error or according to the suggested values by previous scholars [26, 27]. Table 3 presents the optimum values of the genetic parameters adopted in this study.

Table 3. Setting parameters for the proposed GEP model

Parameter	Setting
Function set	+, ×, /, 2√, 3√, 4√, x2, x3, x4
No. of chromosomes	150
Head Size	9
No of genes	3
Linking Function	+
No of constant per gene	3
Mutation rate	0.05
Inversion rate	0.1
Gene recombination rate	0.1
Gene transposition rate	0.1
One-point recombination rate	0.3
Two-point recombination rate	0.3

The proposed model consists of three genes, and each has three constants. The linking functions between genes are addition. The values of the constants in the second and third genes are c2 = 0.64 and c0 = 8.82, respectively. Simple functions are implemented in the proposed model to facilitate the calculations without losing accuracy. Functions used in the model included addition, multiplication, division, square root, cube root, quartic root, and *x* to the power of 2, 3, and 4.

Six input parameters are used to develop the proposed model. The employed parameters are the concrete strength (d0 = f_c), the slab's width-the concentrated load's ratio (d1 = b/b_l), the flexural reinforcements ratio in the longitudinal direction (d2 = ρ), the shear span-effective depth (longitudinal direction) ratio (d3 = a/d), the effective depth of a slab in the longitudinal direction (d4 = d), the slab's width-effective depth (longitudinal direction) ratio (d5 = b/d). The corresponding ET of the proposed model is presented in Figure 5. The GEP formulation of the SS (V_{GEP}) in terms of f_c, b/b_l, ρ, a/d, d, and b/d is given by:

$$V_{GEP} = \left[\sqrt{\frac{f_c}{\left(\frac{b/b_l}{f_c/d} \times \sqrt[3]{\frac{d}{\rho}} \right)}} + \frac{\sqrt{d}}{\left[\left(\frac{(a/d)^3}{\rho} \right) \times \left(0.64 \times \frac{a}{d} \right) + \frac{b}{d} \right]} + \sqrt{\frac{\frac{f_c}{\sqrt[3]{\frac{b/d}{\sqrt{\frac{}{8.82}}}}}}{d}} \right] \times bd \quad (1)$$

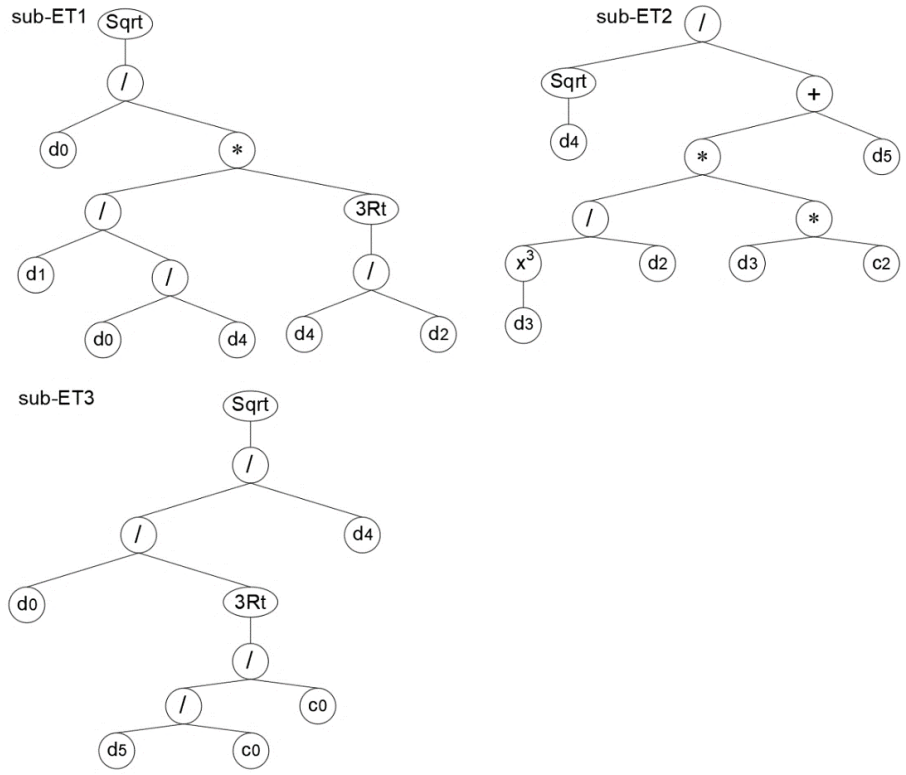

Figure 5. ETs of the proposed model

5. Model Reliability and Comparative Study

Statistical analysis is carried out to evaluate the performance of the proposed model. According to Smith [57], the accuracy of a model is deemed acceptable when it provides a correlation coefficient (R) greater than 0.8, which indicates a robust correlation between the estimated and measured strengths. R is expressed as follows:

$$R = \frac{\sum_{i=1}^{n}(x_i-\bar{x}_i)(y_i-\bar{y}_i)}{\sqrt{\sum_{i=1}^{n}(x_i-\bar{x}_i)^2 \sum_{i=1}^{n}(y_i-\bar{y}_i)^2}} \quad (2)$$

xi and yi are the measured and estimated values, respectively; $\bar{x}_i$, $\bar{y}_i$ are the average of measured and estimated values; and n is the number of points within data. Values of R usually range from zero to one, where the former value indicates no correlation between the measured and estimated strength zero, and the latter indicates the perfect correlation between the measured and estimated strength, respectively.

However, the use of R only is not enough because it is not affected by the variances between the estimated and measured strength [58]. Therefore, other statistical indices must be employed, such as the root mean square error (RMSE) and mean absolute error (MAE) affected by the variances between the estimated and measured strengths. RMSE is the square root of the differences between estimated predictions and tests, while MAE represents the average of the absolute differences between estimated strength and measured ones. The lower values of these indices denote the close agreements between the estimated and measured strengths, while a zero value points to the perfect match between the estimated and measured strengths. RMSE and MAE are expressed as follows:

$$RMSE = \frac{\sqrt{\sum_{i=1}^{n}(x_i-y_i)^2}}{n} \quad (3)$$

$$MAE = \frac{\sum_{i=1}^{n}|x_i-y_i|}{n} \quad (4)$$

The performance of the proposed model is examined for all divisions of the database. It is to ensure its consistency and generality and to avoid overfitting. The R, RMSE, and MAE are computed for the training set, testing set, and the total database. Figure 6 shows comparisons between the estimated strength by the GEP model and measured ones, along with the values of the above-described statistical indices. R is 0.97 for the training set, testing set, and the whole database. RMSE for the training set, testing set, and the entire database are 117.85, 72.85, and 106.44, respectively; MAE for the training set, testing set, and the whole database is 70.71, 42.76, and 62.37, respectively. The R's high value and the low values of both RMSE and MAE indicate that the GEP correlates well with the test results of the whole database and the training and testing sets. These prove to eliminate over-fitting. Such correlation is due to considering all the influencing parameters in the proposed model.

Table 4 presents the values statistical indices of the proposed GEP model and the existing models listed in Table 2 for the whole database. This table demonstrates that the GEP-based model overperforms the other models, which is expected as these models were derived using the test results of heavily reinforced slender beams and ignored the influence of b/d, leading to inconsistent strength estimation when b/d is higher than 1 [59].

Table 4. Performance of the proposed and the existing models

Model Name	R	RMSE	MAE
ACI-318-25 [7]	0.79	278.88	166.17
EC2-French practice [8]	0.64	356.46	212.55
EC2-Dutch practice [8]	0.53	414.56	249.52
AASHTO 2007 [9]	0.78	286.61	172.70
Model Code 2010 [10]	0.73	399.62	257.96
CSCT [11]	0.81	534.29	275.02
Proposed model	0.97	106.44	62.37

The comparisons between the existing models revealed that the ACI-318-25 [7] and the AASHTO 2007 [9] correlate better with the test results than the EC2 [8] (French and Dutch practices) and the Model Code 2010 [10]. It is due to the use of the effective width method (see Figure 6), which was found to have a pronounced effect on the SS estimations, especially for the ratio of the clear shear span-effective depth of a slab greater than 3 (av/d >3) leading to unsafe and scattered strength estimations [5].

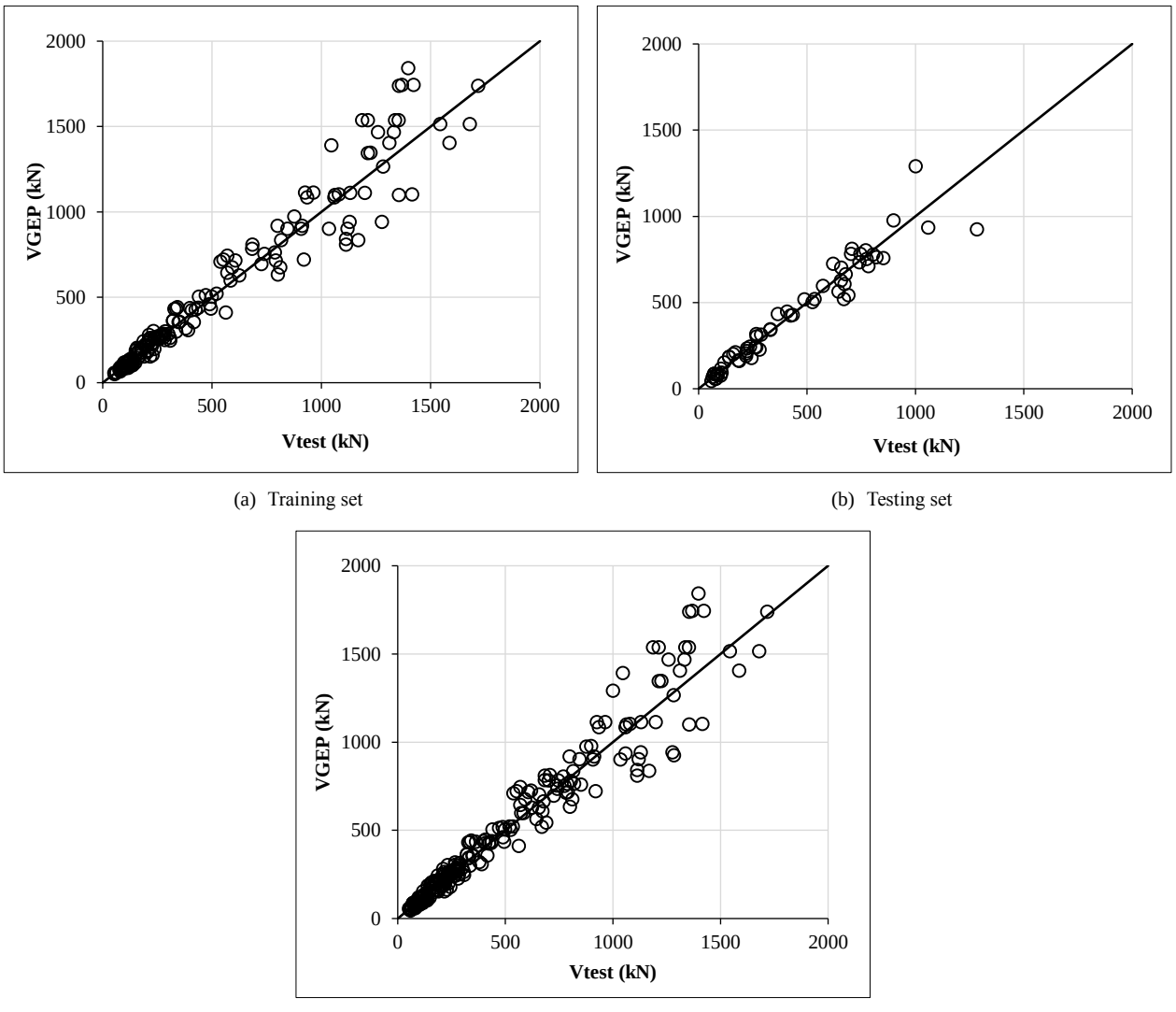

(a) Training set

(b) Testing set

(c) All database

Figure 6. Performance of the GEP model

6. Parametric Study and Sensitivity Analysis

A parametric study is conducted to examine the trend of the GEP model with variation in the input parameters for further validation, where each input is varied while the others are kept constant [60]. The performance of the proposed model is measured by comparing the trends of the estimated strength with the physical behavior of slabs reported in the previous studies.

A set of artificial values is developed for each input parameter within its range in the database. The SS (V_{GEP}) is estimated using the developed data, and this process is repeated for the other input parameters until the model's response for all parameters is determined. Figure 7 shows the trend of estimated strength to the variation of the input parameters, that is, f_c (MPa), b/b_l, ρ (%), a/d, d (mm), and b/d.

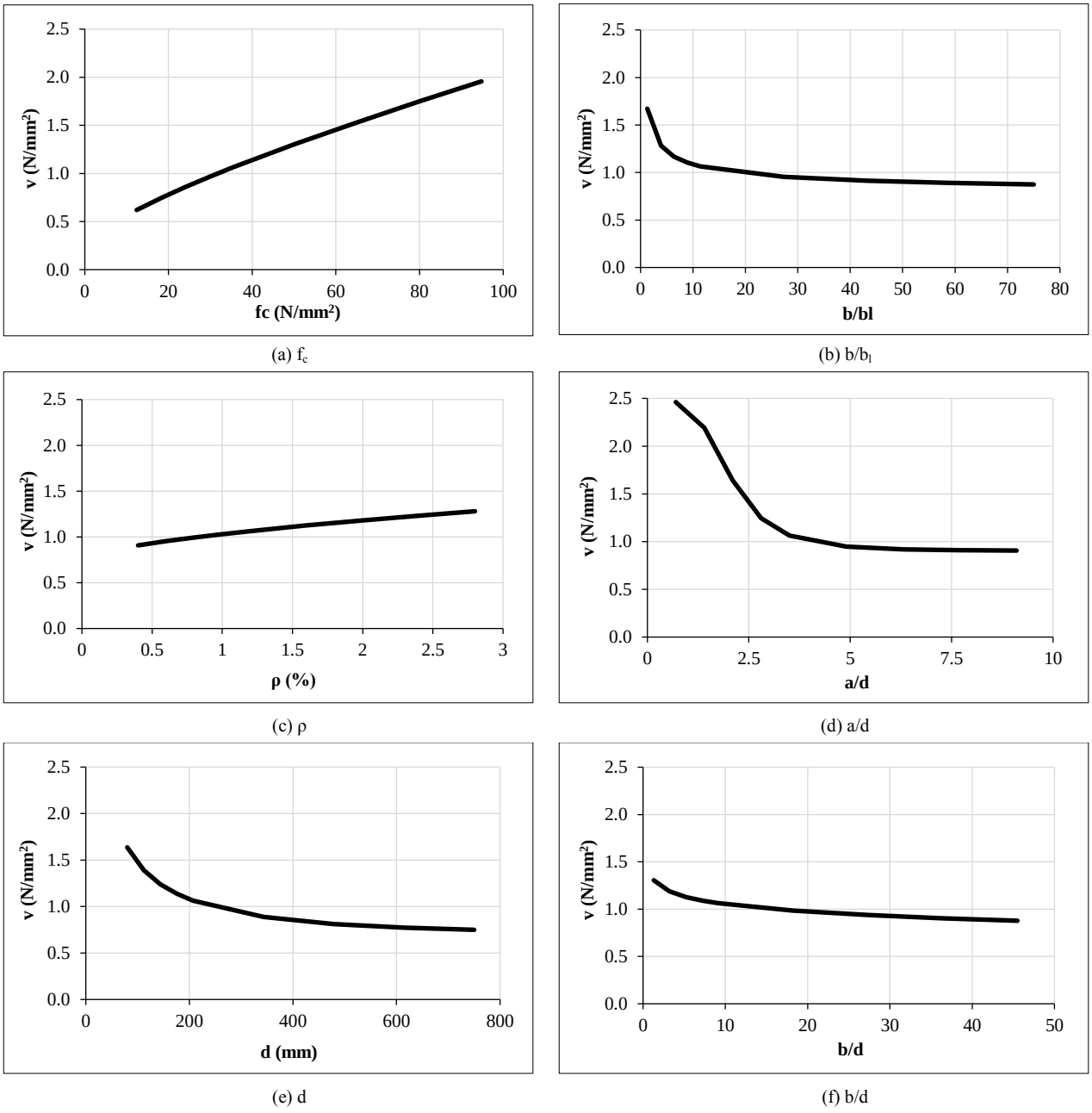

(a) f_c (b) b/b_l

(c) ρ (d) a/d

(e) d (f) b/d

Figure 7. Parametric study of the input parameters used in the GEP model

As inferred from Figure 7, the SS increases with f_c and ρ and decreases with b/b_l, a/d, d, and b/d. The results obtained from the parametric study are in good agreement with the physical behavior reported in previous experimental investigations [1-4, 15, 16, 59]. The trends confirmed the reliability of the GEP model to replicate the main features of the SS of RC one-way slabs under CLs.

The influence of f_c and ρ can be explained by the well-established shear resistance mechanism in RC beams and slabs that consists of three components: concrete compression zone, aggregate interlock, and dowel action, where they co-exist, though they do not develop their full contribution at the same time. The resistance provided by the compression

zone developed first, and the aggregate interlocks contribute only after the formation of the inclined shear crack at the mid-height of the section projecting towards the compression zone, while the dowel action of flexural reinforcement prevents the cracks propagation [61]. The shear contribution of the compression zone depends on the area above the neutral axis and the properties of concrete, and hence, it increases with the f_c. The increase of ρ reduces the crack width and the relative displacement between the cracks' faces, which increases their surface roughness and hence improves the shear resistance of the aggregate interlock. The increase in the SS with the decrease of a/d is due to the development of arch action between the load and the support [62], while the reduction of the SS with the increase of d is related to the size effect [60]. The decrement of the SS with the rise of b/b_l and b/d is due to the reduction in the influence of a/d and the reduction of moment distribution at the supports [16].

A sensitivity analysis is performed to evaluate the contribution of each of the input parameters to the estimated strength. For this purpose, the sensitivity index (SI) of the estimated strength of every input parameter is calculated from the following [63]:

$$N_i = f_{max}(x_i) - f_{min}(x_i) \quad (5)$$

$$SI_i = \frac{N_i}{\sum_{j=1}^{n} N_j} \quad (6)$$

In which, $f_{max}(x_i)$ and $f_{min}(x_i)$ are the maximum and the minimum values of the estimated strength, respectively, with the ith input domain while the rest of the input parameters are set to their mean values within the database.

Table 5 presents the results of the sensitivity analysis. This table indicates that the f_c and a/d have the maximum influence on the SS predicted by the GEP model, which complies with the previous experimental results [1-3] and is comparable to those predicted by the existing models (EC2 [8], Model Code 2010 [10], CSCT [11]). The table also indicates that the estimated SS by the proposed model is less sensitive to ρ, b/d, and b/b_l compared to f_c and a/d. It is hardly surprising because f_c usually enhances the contribution of the concrete compression zone to the SS, and a/d reflects the arch action and direct load transferring mechanism by compression strut [62]. However, the ACI-318-25 [7] and the AASHTO [9] are sensitive to f_c only because it is the only parameter considered in the calculation of the SS. It is important to note that the obtained results regarding the influence of ρ and b/d are comparable to those reported earlier [20, 64], suggesting a lower effect on the SS compared to other parameters.

Table 5. Sensitivity index of the input parameters

Design code	f_c	b/b_l	ρ	a/d	d	b/d
ACI-318-25 [7]	100	0	0	0	0	0
EC2 [8]	11.28	0	8.51	30.12	25.05	25.05
AASHTO [9]	100	0	0	0	0	0
Model Code 2010 [10]	19.38	0	0	63.91	0	16.71
CSCT [11]	27.18	0	0	24.27	24.27	24.27
Proposed model	25.4	15.9	7.5	25.0	18.1	8.9

The influence of a/d on the SS is acknowledged by the GEP models and the existing models while ignored by the ACI-318-25 [7] and AASHTO [9]. This parameter plays a significant role in evaluating existing structures because the SS enhancement associated with the arch action could save the replacement cost of these structures in certain conditions. In addition, despite the comprehensive dataset, the entire slabs considered are rectangular. The GEP model can be applied to estimate the SS of skewed slabs, considering the influence of skew angle as one of the input parameters in the presence of test results of such slabs failing by one-way shear.

7. Conclusion

This paper presents an empirical model to estimate the SS of RC one-way slabs subjected to CLs. It is derived based on the GEP technique relating the SS to experimental results instead of beforehand assumptions used in the development of conventional models to produce a closed-form expression, considering the influence of f_c, b/b_l, ρ, a/d, d, and b/d in the SS estimations that can be utilized as a design tool. A total of 238 RC slabs tested under CLs near the supports failed in shear are collected from the literature to train and test the GEP model. The latter showed good agreement with the test results and better performance than the considered existing models (ACI-318-25 [7], the EC2 [8] (the French and Dutch approaches), the AASHTO 2007 [9], and the Model Code 2010 [10], and the CST [11]). Moreover, a parametric study is performed for additional verification. The results demonstrated the consistency of the proposed closed-form expression in mimicking physical behavior, where the SS increases with f_c and ρ and decreases with b/b_l, a/d, d, and b/d. A sensitivity analysis is performed to examine the influence of the aforesaid parameters in the SS calculations. The results indicated that the SS is more sensitive to f_c and a/d than other parameters.

8. Declarations

8.1. Author Contributions

Conceptualization, A.F.A; methodology, A.F.A; software, A.F.A.; validation, O.S.F. and Z.N.M.T.; resources, O.S.F. and Z.N.M.T; writing—original draft preparation, A.F.A.; writing—review and editing, A.F.A.; visualization, A.F.A, O.S.F., and Z.N.M.T. All authors have read and agreed to the published version of the manuscript.

8.2. Data Availability Statement

The database used in the analysis is available in the article.

8.3. Funding

The authors received no financial support for the research, authorship, and/or publication of this article.

8.4. Conflicts of Interest

The authors declare no conflict of interest.

9. References

[1] Natário, F., Fernández Ruiz, M., & Muttoni, A. (2014). Shear strength of RC slabs under concentrated loads near clamped linear supports. Engineering Structures, 76, 10–23. doi:10.1016/j.engstruct.2014.06.036.

[2] Lantsoght, E. O. L., Cor van der Veen, & Walraven, J. C. (2013). Shear in one-way slabs under concentrated load close to support. ACI Structural Journal, 110(2), 275–284. doi:10.14359/51684407.

[3] Reissen, K., Classen, M., & Hegger, J. (2018). Shear in reinforced concrete slabs—Experimental investigations in the effective shear width of one-way slabs under concentrated loads and with different degrees of rotational restraint. Structural Concrete, 19(1), 36–48. doi:10.1002/suco.201700067.

[4] Lantsoght, E. O. L., van der Veen, C., Walraven, J., & de Boer, A. (2013). Recommendations for the Shear Assessment of Reinforced Concrete Slab Bridges from Experiments. Structural Engineering International, 23(4), 418–426. doi:10.2749/101686613x13627347100239.

[5] Halvonik, J., Vidaković, A., & Vida, R. (2020). Shear Capacity of Clamped Deck Slabs Subjected to a Concentrated Load. Journal of Bridge Engineering, 25(7), 04020037. doi:10.1061/(asce)be.1943-5592.0001564.

[6] Henze, L., Rombach, G. A., & Harter, M. (2020). New approach for shear design of reinforced concrete slabs under concentrated loads based on tests and statistical analysis. Engineering Structures, 219. doi:10.1016/j.engstruct.2020.110795.

[7] ACI 318-25. (2019). ACI 318-25: Building Code Requirements for Structural Concrete (ACI 318-25) and Commentary (ACI 318R-19). American Concrete Institute (ACI), Farmington Hills, United States.

[8] EN 1992-1-1: 2004. (2004). Eurocode 2 Design of Concrete Structures—Part 1-1 General Rules and Rules for Buildings. European Committee for Standardization, Brussel, Belgium.

[9] AASHTO. (2007). LRFD bridge design specifications. American Association of State Highway and Transportation Officials, Washington, United States.

[10] Fédération Internationale du Béton (fib). (2012). fib model code for concrete structures. Bulletin 65, Ernst & Sohn Fédération Internationale du Béton, Lausanne, Switzerland.

[11] Muttoni, A., & Ruiz, M. F. (2008). Shear strength of members without transverse reinforcement as function of critical shear crack width. ACI Structural Journal, 105(2), 163–172. doi:10.14359/19731.

[12] Lantsoght, E. O. L., van der Veen, C., Walraven, J., & de Boer, A. (2015). Experimental investigation on shear capacity of reinforced concrete slabs with plain bars and slabs on elastomeric bearings. Engineering Structures, 103, 1–14. doi:10.1016/j.engstruct.2015.08.028.

[13] Lantsoght, E. O. L., van der Veen, C., Walraven, J. C., & de Boer, A. (2015). Transition from one-way to two-way shear in slabs under concentrated loads. Magazine of Concrete Research, 67(17), 909–922. doi:10.1680/macr.14.00124.

[14] Bui, T. T., Abouri, S., Limam, A., NaNa, W. S. A., Tedoldi, B., & Roure, T. (2017). Experimental investigation of shear strength of full-scale concrete slabs subjected to concentrated loads in nuclear buildings. Engineering Structures, 131, 405–420. doi:10.1016/j.engstruct.2016.10.045.

[15] Furuuchi, H., Takahashi, Y., Ueda, T., & Kakuta, Y. (1998). Effective width for shear failure of RC deep slabs. Transactions of the Japan Concrete Institute, 20, 209–216.

[16] Lantsoght, E. O. L., Van Der Veen, C., De Boer, A., & Walraven, J. C. (2014). Influence of width on shear capacity of reinforced concrete members. ACI Structural Journal, 111(6), 1441–1449. doi:10.14359/51687107.

[17] Lantsoght, E. (2012). Shear in reinforced concrete slabs under concentrated loads close to the support. Ph.D. Thesis, Delft University of Technology, Delft, Netherlands.

[18] Lantsoght, E. O. L., van der Veen, C., de Boer, A., & Walraven, J. (2015). Proposal for the extension of the Eurocode shear formula for one-way slabs under concentrated loads. Engineering Structures, 95, 16–24. doi:10.1016/j.engstruct.2015.03.055.

[19] Lantsoght, E. O. L., Van Der Veen, C., De Boer, A., & Alexander, S. D. B. (2017). Extended strip model for reinforced concrete slabs under concentrated loads. ACI Materials Journal, 114(2), 565–574. doi:10.14359/51689462.

[20] Abambres, M., & Lantsoght, E. O. L. (2020). Neural network-based formula for shear capacity prediction of one-way slabs under concentrated loads. Engineering Structures, 211(110501). doi:10.1016/j.engstruct.2020.110501.

[21] Kongwang, N., Takeda, K., Sato, Y., & Pheinsusom, P. (2024). Fatigue life prediction method for reinforced concrete deck slabs subjected to repeated moving wheel loads and failing in shear. Structural Concrete, 25(6), 4324-4339. doi:10.1002/suco.202400114.

[22] Fernández, P. G., Marí, A., & Oller, E. (2023). Theoretical prediction of the shear strength of reinforced concrete slabs under concentrated loads close to linear supports. Structure and Infrastructure Engineering, 19(7), 890–903. doi:10.1080/15732479.2021.1988990.

[23] Huber, T., Huber, P., Wolfger, H., Vill, M., & Kollegger, J. (2024). Shear tests on full-scale bridge slabs with bent-up reinforcing bars. Engineering Structures, 308, 117966. doi:10.1016/j.engstruct.2024.117966.

[24] Lipari, A. (2024). A review of design and assessment methods for skew concrete slabs. Bridge Maintenance, Safety, Management, Digitalization and Sustainability, 3904–3912, CRC Press, Boca Raton, United States. doi:10.1201/9781003483755-461.

[25] Setiawan, A., Cantone, R., Fernández Ruiz, M., & Muttoni, A. (2024). Verification of shear failures of cantilever bridge deck slabs subjected to concentrated loads. Engineering Structures, 303(117491). doi:10.1016/j.engstruct.2024.117491.

[26] Abdulkathum, S., Al-Shaikhli, H. I., Al-Abody, A. A., & Hashim, T. M. (2023). Statistical Analysis Approaches in Scour Depth of Bridge Piers. Civil Engineering Journal (Iran), 9(1), 143–153. doi:10.28991/CEJ-2023-09-01-011.

[27] Al-Bayati, A. F. (2023). Shear Strength of Circular and Rectangular Reinforced Concrete Columns. KSCE Journal of Civil Engineering, 27(5), 2073–2088. doi:10.1007/s12205-023-0027-y.

[28] Chen, G., Cheng, X., Diao, M., Li, Y., & Lu, Y. (2025). Progressive collapse resistance of one-way wet-connected precast concrete beam-slab-column substructures: Experimental and numerical investigations. Engineering Structures, 344, 121288. doi:10.1016/j.engstruct.2025.121288.

[29] Shrif, M., Al-Sadoon, Z. A., Barakat, S., Habib, A., & Mostafa, O. (2024). Optimizing Gene Expression Programming to Predict Shear Capacity in Corrugated Web Steel Beams. Civil Engineering Journal, 10(5), 1370-1385. doi:10.28991/CEJ-2024-010-05-02.

[30] Fang, I. K., Tsui, C. K. T., Burns, N. H., & Klingner, R. E. (1990). Load capacity of isotropically reinforced, cast-in-place and precast panel bridge decks. PCI Journal, 35(4), 104–113. doi:10.15554/pcij.07011990.104.113.

[31] Regan, P. E., & Rezai-Jorabi, H. (1988). Shear Resistance of One-Way Slabs under Concentrated Loads. ACI Structural Journal, 85(2), 150–157. doi:10.14359/2704.

[32] Vaz Rodrigues, R., Muttoni, A., & Burdet, O. (2006). Large scale tests on bridge slabs cantilevers subjected to traffic loads. Proceedings of the 2nd international Congress, Fédération Internationale du Béton, 5-8 June, 2006, Naples, Italy.

[33] Kani, M. W., Huggins, M. W., & Wittkopp, R. R. (1979). Kani on shear in reinforced concrete. University of Toronto Press, Toronto, Canada.

[34] Olonisakin, A. A., & Alexander, S. D. B. (1999). Mechanism of shear transfer in a reinforced concrete beam. Canadian Journal of Civil Engineering, 26(6), 810–817. doi:10.1139/l99-044.

[35] Regan, P. E. (1982). Shear resistance of concrete slabs at concentrated loads close to supports. Polytechnic of Central London, London, United Kingdom.

[36] Reißen, K., & Hegger, J. (2013). Experimental investigations on the effective width for shear force of single-span roadway slabs. Beton- Und Stahlbetonbau, 108(2), 96–103. doi:10.1002/best.201200064. (In German).

[37] Reißen, K., & Hegger, J. (2013). Experimental investigations into the shear force behavior of cantilevered road slabs under wheel loads. Beton- Und Stahlbetonbau, 108(5), 315–324. doi:10.1002/best.201200072. (In German).

[38] Graf, O. (1933). Experiments on the capacity of concrete slabs subjected to concentrated loads close to a support. Deutscher Ausschuss für Eisenbeton, 73, 10-16. (In German).

[39] Heger, F. J., & McGrath, T. J. (1982). Design method for reinforced concrete pipe and box sections. Simpson Gumpertz and Heger, Inc, Waltham, United States.

[40] Coin A, & Thonier, H. (2007). Shear experiments on reinforced concrete slabs. Annales du baˆtiment et des travaux publics 59(1), 7-16. (In French).

[41] Rajagopalan, K. S., & Ferguson, P. M. (1968). Exploratory shear tests emphasizing percentage of longitudinal steel. Journal Proceedings 65(8), 634-638. doi:10.14359/7501.

[42] Serna-Ros, P., Fernandez-Prada, M. A., Miguel-Sosa, P., & Debb, O. A. R. (2002). Influence of stirrup distribution and support width on the shear strength of reinforced concrete wide beams. Magazine of Concrete Research, 54(3), 181–191. doi:10.1680/macr.2002.54.3.181.

[43] Leonhardt, F., & Walther, R. (1962). The Stuttgart shear tests, 1961: contributions to the treatment of the problems of shear in reinforced concrete construction. Cement & Concrete Association, London, United Kingdom.

[44] Aster, H., & Koch, R. (1974). Shear capacity of thick reinforced concrete slabs. Beton-U Stahlbetonbau, 69(11). (In German).

[45] Cullington, D. W., Daly, A. F., & Hill, M. E. (1996). Assessment of reinforced concrete bridges: Collapse tests on Thurloxton underpass. Bridge Management: Proceedings of the Third International Conference, 14-17 April 1996, Guildford, United Kingdom.

[46] Cossio R, D., J, M., P.L, G., & J.G, M. (1962). Shear and Diagonal Tension. ACI Journal Proceedings, 59(3), 1323–1339. doi:10.14359/7921.

[47] Reineck, K. H., Koch, R., & Schlaich, J. (1978). Shear Tests on Reinforced concrete beams with axial compression for offshore structures. Institut für Massivbau, Universität Stuttgart, Stuttgart, Germany.

[48] Jäger, T. (2002). Shear strength and deformation capacity of reinforced concrete slabs. Proceedings of the 4th International Ph.D. Symposium in Civil Engineering. Munich, Germany.

[49] Ja¨ger T. (2005). Experiments on the Shear and Deformation Capacity of Reinforced Concrete Slabs. ETH Zurich, Zurich, Switzerland. (In German).

[50] Ja¨ger T. (2007). Shear and Deformation Capacity of Reinforced Concrete Slabs. PhD Thesis, ETH Zurich, Zurich, Switzerland. (In German).

[51] Rombach, G., & Latte, S. (2008). Shear resistance of bridge decks without shear reinforcement. Tailor Made Concrete Structures, 125–125. doi:10.1201/9781439828410.ch86.

[52] Rombach, G. A., & Latte, S. (2008). Shear resistance of bridge decks without shear reinforcement. Proceedings of the International fib Symposium, 19-21 May 2008, Amsterdam, Netherlands.

[53] Lantsoght, E. O. L., Van Der Veen, C., Walraven, J. C., & De Boer, A. (2015). Database of wide concrete members failing in shear. Magazine of Concrete Research, 67(1), 33–52. doi:10.1680/macr.14.00137.

[54] Al-Bayati, A. F. (2023). Torsion Strength Prediction of Reinforced Concrete Beams. International Review of Civil Engineering, 14(2), 153–163. doi:10.15866/irece.v14i2.22853.

[55] Koza, J. R. (1992). Genetic programming: On the programming of computers by means of natural selection. Biosystems, 33(1), 69–73. doi:10.1016/0303-2647(94)90062-0.

[56] Ferreira, C. (2002). Gene Expression Programming in Problem Solving. Soft Computing and Industry, Springer, London, United Kingdom. doi:10.1007/978-1-4471-0123-9_54.

[57] Smith, G. N. (1986). Probability and Statistics in Civil Engineering. Collins professional and technical books, London, United Kingdom.

[58] Patiño-Mora, K., Santa María, H., & Jünemann, R. (2025). Experimental assessment of reinforced concrete squat walls with high-strength lightweight concrete. Materials and Structures, 58(7), 1-18. doi:10.1617/s11527-025-02756-0.

[59] Conforti, A., Minelli, F., & Plizzari, G. A. (2017). Influence of width-to-effective depth ratio on shear strength of reinforced concrete elements without web reinforcement. ACI Structural Journal, 114(4), 995–1006. doi:10.14359/51689681.

[60] Al-Bayati, A. F., & Taki, Z. N. M. (2024). Shear strength prediction of steel fiber reinforced concrete beams without transverse reinforcements. Asian Journal of Civil Engineering, 25(2), 1857–1875. doi:10.1007/s42107-023-00882-0.

[61] Theodorakopoulos, D. D., & Swamy, R. N. (2002). Ultimate punching shear strength analysis of slab–column connections. Cement and Concrete Composites, 24(6), 509–521. doi:10.1016/s0958-9465(01)00067-1.

[62] Al-Bayati, A. F. (2018). Alternative Strut and Tie Model for Reinforced Concrete Deep Beams. Al-Nahrain Journal for Engineering Sciences, 21(1), 86. doi:10.29194/njes21010086.

[63] Gandomi, A. H., Yun, G. J., & Alavi, A. H. (2013). An evolutionary approach for modeling of shear strength of RC deep beams. Materials and Structures/Materiaux et Constructions, 46(12), 2109–2119. doi:10.1617/s11527-013-0039-z.

[64] de Sousa, A. M. D., Lantsoght, E. O. L., & El Debs, M. K. (2021). One-way shear strength of wide reinforced concrete members without stirrups. Structural Concrete, 22(2), 968–992. doi:10.1002/suco.202000034.

Appendix I

Table A1. Geometrical and material properties used to train the GEP model

Source	Slab No.	b (mm)	d (mm)	a/d	b/b_l	b/d	f_c (MPa)	ρ (%)	V_{test} (kN)	V_{GEP} (kN)	V_{GEP}/V_{test}
[1]	S1T1	2500	265	2.26	12.50	9.43	35.8	0.996	799	918.4	1.15
	S1T2	2500	265	2.26	12.50	9.43	35.8	0.996	912	918.4	1.01
	S2T1	2500	265	2.26	8.33	9.43	34.5	0.996	1129	941.4	0.83
	S2T4	2500	265	2.26	8.33	9.43	34.5	0.996	1276	941.4	0.74
	S3T1	2500	265	2.26	8.33	9.43	51.6	0.996	1131	1112.2	0.98
	S3T4	2500	265	2.26	8.33	9.43	51.6	0.996	1199	1112.2	0.93
	S4T1	2500	265	2.26	8.33	9.43	51.7	0.996	964	1113.2	1.15
	S4T2	2500	265	2.26	8.33	9.43	51.7	0.996	925	1113.2	1.20
	S5T1	2500	265	1.51	8.33	9.43	48.2	0.996	1679	1514.2	0.90
	S5T4	2500	265	1.51	8.33	9.43	48.2	0.996	1544	1514.2	0.98
	S6T1	2500	265	1.51	8.33	9.43	50.6	0.996	1353	1537.4	1.14
	S6T2	2500	265	1.51	8.33	9.43	50.6	0.996	1337	1537.4	1.15
	S6T4	2500	265	1.51	8.33	9.43	50.6	0.996	1213	1537.4	1.27
	S6T5	2500	265	1.51	8.33	9.43	50.6	0.996	1187	1537.4	1.30
	S7T2	2500	265	2.26	8.33	9.43	82.1	0.996	1046	1390.5	1.33
	S8T1	2500	265	2.26	8.33	9.43	77	0.996	1226	1345.6	1.10
	S8T2	2500	265	2.26	8.33	9.43	77	0.996	1213	1345.6	1.11
	S9T1	2500	265	1.51	12.50	9.43	81.7	0.996	1355	1738.4	1.28
	S9T4	2500	265	1.51	12.50	9.43	81.7	0.996	1717	1738.4	1.01
	S10T4	2500	265	1.51	12.50	9.43	82.4	0.996	1422	1743.8	1.23
	S10T5	2500	265	1.51	12.50	9.43	82.4	0.996	1368	1743.8	1.27
[30]	1	6100	134	9.10	12.01	45.52	29	0.426	569	643.5	1.13
	2	6100	134	9.10	3.53	45.52	29	0.426	816	834.9	1.02
[31]	1	400	83	5.42	5.33	4.82	31	1.66	62.5	58.6	0.94
	2	600	83	5.42	8.00	7.23	31	1.58	85	77.5	0.91
	3	800	83	5.42	10.67	9.64	31	1.54	97.5	94.7	0.97
	4	400	83	5.42	4.00	4.82	23	1.66	54.5	50.5	0.93
	5	600	83	5.42	6.00	7.23	23	1.58	80	66.7	0.83
	6	800	83	5.42	8.00	9.64	23	1.54	96.5	81.6	0.85
	10	400	83	5.42	4.00	4.82	27.4	1.66	52.5	57.2	1.09
	11	400	83	5.42	4.00	4.82	27.4	1.66	55	57.2	1.04
	12	600	83	5.42	6.00	7.23	27.4	1.58	76	75.4	0.99
	13	600	83	5.42	6.00	7.23	27.4	1.58	79.5	75.4	0.95
	14	800	83	5.42	8.00	9.64	25.4	1.54	92.5	87.3	0.94
	15	800	83	6.63	8.00	9.64	25.3	1.54	85	86.2	1.01
	16	800	83	5.42	8.00	9.64	25.6	1.54	108	87.8	0.81
	17	1000	83	5.42	13.33	12.05	25.4	1.51	90	97.2	1.08
	18	1000	83	5.42	10.00	12.05	25.6	1.51	120	102.7	0.86
	19	1000	83	5.42	10.00	12.05	23.8	1.51	111	97.8	0.88
	20	1000	83	5.42	10.00	12.05	25.3	1.51	122.5	101.9	0.83
	21	1200	80	5.63	12.00	15.00	31.3	1.64	117.5	131.9	1.12
	22	1200	80	5.63	12.00	15.00	30.3	1.64	121.5	129.0	1.06
	23	1200	80	5.63	12.00	15.00	29	1.64	125	125.2	1.00
	24	1200	80	5.63	4.00	15.00	31.7	1.64	150	170.7	1.14
	25	1200	80	6.88	12.00	15.00	24.8	1.64	105.8	111.5	1.05
	26	1200	80	4.38	12.00	15.00	24.4	1.64	137.5	114.7	0.83
	14R	800	83	5.42	8.00	9.64	25.4	1.54	77	87.3	1.13
	15R	800	83	5.42	8.00	9.64	25.3	1.54	86	87.1	1.01
	16R	800	83	5.42	8.00	9.64	25.6	1.54	116.5	87.8	0.75
	17R	1000	83	5.42	10.00	12.05	25.4	1.51	137.5	102.2	0.74
	19R	1000	83	5.42	10.00	12.05	23.8	1.51	85	97.8	1.15
	20R	1000	83	5.42	10.00	12.05	25.3	1.51	132.5	101.9	0.77

[2]	SN1	3000	152	4.96	7.50	19.74	30.3	1.32	489	459.4	0.94
	SN1	3000	152	4.96	7.50	19.74	28.3	1.32	437	438.6	1.00
	SN2	3000	152	5.96	7.50	19.74	29.5	1.32	341	442.1	1.30
	SN4	3000	152	5.96	7.50	19.74	28.8	1.32	494	434.8	0.88
	SN5	3000	152	5.96	7.50	19.74	28.7	1.32	335	433.7	1.29
	SN6	3000	152	6.96	7.50	19.74	28.9	1.32	327	431.8	1.32
[16]	BS1T2	500	265	2.26	2.50	1.89	81.5	0.948	562	410.6	0.73
	BS2T1	500	265	1.51	2.50	1.89	88.6	0.948	552	720.9	1.31
	BS2T2	500	265	1.51	2.50	1.89	88.6	0.948	919	720.9	0.78
	BS3T2	500	265	2.26	2.50	1.89	91	0.948	399	437.5	1.10
	BM1T1	1000	265	2.26	5.00	3.77	81.5	0.948	811	676.0	0.83
	BM1T2	1000	265	2.26	5.00	3.77	81.5	0.948	591	676.0	1.14
	BM2T1	1000	265	1.51	5.00	3.77	88.6	0.948	1062	1098.8	1.03
	BM2T2	1000	265	1.51	5.00	3.77	88.6	0.948	1354	1098.8	0.81
	BM3T1	1000	265	2.26	5.00	3.77	91	0.948	607	716.8	1.18
	BM3T2	1000	265	2.26	5.00	3.77	91	0.948	791	716.8	0.91
	BL1T1	1500	265	2.26	7.50	5.66	81.5	0.948	844	902.0	1.07
	BL1T2	1500	265	2.26	7.50	5.66	81.5	0.948	1119	902.0	0.81
	BL2T1	1500	265	1.51	7.50	5.66	94.8	0.948	1311	1404.7	1.07
	BL2T2	1500	265	1.51	7.50	5.66	94.8	0.948	1586	1404.7	0.89
	BL3T1	1500	265	2.26	7.50	5.66	81.4	0.948	907	901.4	0.99
	BL3T2	1500	265	2.26	7.50	5.66	81.4	0.948	1035	901.4	0.87
	BX1T1	2000	265	2.26	10.00	7.55	81.4	0.948	1080	1102.4	1.02
	BX1T2	2000	265	2.26	10.00	7.55	81.4	0.948	1415	1102.4	0.78
	BX2T1	2000	265	1.51	10.00	7.55	70.4	0.948	1259	1467.2	1.17
	BX2T2	2000	265	1.51	10.00	7.55	70.4	0.948	1332	1467.2	1.10
	BX3T1	2000	265	2.26	10.00	7.55	78.8	0.948	935	1084.9	1.16
	BX3T2	2000	265	2.26	10.00	7.55	78.8	0.948	1059	1084.9	1.02
[32]	DR1a	10000	306	4.56	33.33	32.68	39.1	0.79	1397	1842.9	1.32
[33]	271	611	269	6.07	6.11	2.27	27	2.75	217	153.3	0.71
	272	611	271	5.02	6.11	2.25	27	2.73	228	163.4	0.72
	273	612	271	4.01	6.12	2.26	27.2	2.72	206	189.4	0.92
	274	612	270	3.02	6.12	2.27	27.2	2.73	250	270.9	1.08
[34]	CB1(b)	750	128	3.32	75.00	5.86	32.5	1.04	129	102.2	0.79
	CB2	750	128	2.93	75.00	5.86	32.5	1.04	130	109.9	0.85
	RB1	750	128	3.32	75.00	5.86	32.5	1.04	123	102.2	0.83
	RB2	750	128	2.93	75.00	5.86	32.5	1.04	128	109.9	0.86
[35]	1-SS	1200	84	2.62	12.00	14.29	24	0.602	97	119.3	1.23
	1-CS	1200	84	2.92	12.00	14.29	24	0.602	118	115.1	0.98
	2-SS	1200	84	2.14	12.00	14.29	22.2	0.602	110	124.9	1.14
	2-CS	1200	84	2.44	12.00	14.29	22.2	0.602	148	117.5	0.79
	3-SS	1200	84	1.67	12.00	14.29	29	0.602	171	160.1	0.94
	4-SS	1200	84	1.43	12.00	14.29	33.9	0.602	206	181.6	0.88
	5-SS	1200	84	2.14	12.00	14.29	29.3	0.602	160	145.0	0.91
	6-SS	1200	84	2.74	6.00	14.29	26.6	0.602	128	140.2	1.10
	6-CS	1200	84	3.04	6.00	14.29	26.6	0.602	125	136.5	1.09
	7-SS	1200	84	1.67	12.00	14.29	35.4	0.602	176	177.2	1.01
	7-CS	1200	84	2.44	12.00	14.29	35.4	0.602	189	153.9	0.81
[15]	A-10–20	500	160	1.75	10.00	3.13	20.2	2.23	186	242.3	1.30
	A-10–30	500	160	1.75	10.00	3.13	23.8	2.23	210	250.0	1.19
	A-20–10	500	160	1.75	10.00	3.13	19.6	2.23	215	241.0	1.12
	A-30–10	500	160	1.75	10.00	3.13	23.8	2.23	284	250.0	0.88
	B-10–10	650	160	1.75	13.00	4.06	29.4	2.29	232	302.8	1.31
	C-10–10	500	160	1.25	10.00	3.13	34.6	2.23	320	362.0	1.13
	C-20–10	500	160	1.25	10.00	3.13	32.1	2.23	350	357.2	1.02
	C-30–10	500	160	1.25	10.00	3.13	31.5	2.23	417	356.1	0.85
	C-10–20	500	160	1.25	10.00	3.13	36.4	2.23	322	365.4	1.13
	C-10–30	500	160	1.25	10.00	3.13	30.7	2.23	347	354.5	1.02
	D-10–10	500	160	2.25	10.00	3.13	35.2	2.23	179	195.2	1.09

[36, 37]	1501TV	1500	240	4.17	3.75	6.25	37.7	0.98	407	425.6	1.05
	1502TV	1500	240	4.17	3.75	6.25	38.2	0.98	425	429.4	1.01
	2501TV	2500	240	4.17	6.25	10.42	27.9	0.98	498	503.7	1.01
	2502TV	2500	240	4.17	6.25	10.42	29.5	0.98	520	521.7	1.00
	3501TV	3500	240	4.17	8.75	14.58	35.9	0.98	739	754.2	1.02
	3502TV	3500	240	4.17	8.75	14.58	38.2	0.98	683	784.6	1.15
	350a11TV	3500	240	5.42	8.75	14.58	39.6	0.98	787	763.9	0.97
	350a12TV	3500	240	2.92	8.75	14.58	41.3	0.98	876	973.8	1.11
	350a21TV	3500	240	5.42	8.75	14.58	29.5	0.98	624	628.1	1.01
	350a22TV	3500	240	2.92	8.75	14.58	29	0.98	684	809.0	1.18
	Tb11TV	3500	240	4.75	8.75	14.58	37	0.98	569	744.7	1.31
	Tb21TV	3500	240	4.75	8.75	14.58	34.3	0.98	538	708.7	1.32
	505b	1524	406	2.25	4.28	3.75	25.7	0.68	1168	835.9	0.72
	506a	1524	406	2.25	4.28	3.75	23.1	0.68	1112	809.2	0.73
	506b	1524	406	2.25	4.28	3.75	26.3	0.68	1112	841.9	0.76
[38]	1243-a1	2000	115	1.30	20.00	17.39	16.6	0.65	280	267.6	0.96
	1243-a2	2000	115	2.17	20.00	17.39	19.1	0.65	193	221.6	1.15
	1243-b1	2000	115	0.65	20.00	17.39	19.1	0.65	336	299.4	0.89
	1244-a1	2004	104	1.92	20.04	19.27	12.7	1.14	236	198.1	0.84
	1244-a2	2004	104	2.40	20.04	19.27	13.3	1.14	161	178.6	1.11
	1245-a1	2404	106	1.89	24.04	22.68	23.7	1.52	285	300.6	1.05
	1245-a2	2404	106	2.36	24.04	22.68	23.6	1.52	211	279.9	1.33
[39]	SW9–0A	914	184	3.24	36.56	4.97	48.5	0.62	168	194.3	1.16
	SW9–0B	914	190	3.14	36.56	4.81	48.5	0.6	156	200.2	1.28
	SW9–6A-15	914	188	2.03	36.56	4.86	48.5	0.61	268	280.8	1.05
	SW9–0B-15	914	186	2.05	36.56	4.91	48.5	0.62	271	276.6	1.02
	SW9M-0A	914	197	3.19	36.56	4.64	48.5	0.61	156	204.6	1.31
	SW9M-0B	914	185	3.23	36.56	4.94	48.5	0.62	174	195.2	1.12
	SW9M-0A-15	914	190	2.01	36.56	4.81	48.5	0.6	300	285.8	0.95
	SW9M-0B-15	914	174	2.19	36.56	5.25	48.5	0.66	308	245.9	0.80
	SW14–0A	914	191	3.13	36.56	4.79	49	0.93	197	216.9	1.10
	SW14–0B	914	186	3.21	36.56	4.91	49	0.96	196	210.9	1.08
	SW18–0A	914	184	3.25	36.56	4.97	48.3	1.24	203	215.8	1.06
	SW18–0B	914	180	3.31	36.56	5.08	48.3	1.27	223	210.8	0.95
	SW18–0A-15	914	179	2.13	36.56	5.11	48.3	1.28	379	319.1	0.84
	SW18–0B-15	914	176	2.17	36.56	5.19	48.3	1.3	390	307.4	0.79
[40]	1	2500	85	4.35	12.50	29.41	25.8	1.072	222	226.9	1.02
	2	2500	85	4.35	12.50	29.41	30.4	1.589	235	262.8	1.12
	5	2500	85	4.35	12.50	29.41	30.2	2.15	264	270.0	1.02
	5bis	2500	85	4.35	12.50	29.41	30.2	2.15	269	270.0	1.00
	6	2500	85	4.35	12.50	29.41	30.2	1.662	307	262.9	0.86
	6bis	2500	85	4.35	12.50	29.41	30.2	1.662	216	262.9	1.22
	AT-2/1000N	1002	438	2.97	6.59	2.29	37.9	0.911	440	504.6	1.15
	AT-2/1000W	1002	439	2.96	6.59	2.28	39	0.909	471	513.2	1.09
	AT-2/3000	3005	440	2.95	19.77	6.83	40.6	0.908	1282	1265.9	0.99
	AT-3/N1	697	307	3.39	4.59	2.27	37.5	0.93	238	256.5	1.08
	AT-3/N2	706	306	3.40	4.64	2.31	37.1	0.93	259	256.3	0.99
	AT-3/T1	700	306	3.40	4.61	2.29	37.8	0.93	253	257.4	1.02
	AT-3/T2	706	307	3.39	4.64	2.30	37.1	0.93	249	257.4	1.03
	AX7	704	287	3.62	4.63	2.45	41	1.04	250.55	256.4	1.02
	AX6	703	288	3.61	4.63	2.44	41	1.73	282.51	285.6	1.01
	AX8	705	289	3.60	4.64	2.44	41	1.72	272.05	287.2	1.06
	AW1	1170	538	3.44	3.84	2.17	36.9	0.79	585	598.1	1.02
	AW4	1168	506	3.66	3.83	2.31	39.9	1.69	725	695.4	0.96
	AW8	1169	507	3.65	7.69	2.31	39.4	1.69	800	633.7	0.79
[41]	S-15	761	269	4.16	7.61	2.83	33	0.63	151	189.9	1.26

Table A2. Geometrical and material properties used to test the GEP model

Source	Slab No.	b (mm)	d (mm)	a/d	b/b_l	b/d	f_c (MPa)	ρ (%)	V_{test} (kN)	V_{GEP} (kN)	$V_{GEP/Vtest}$
[3]	S5B-3	500	240	4.20	1.25	2.08	33.7	0.98	140	184.6	1.32
	S5D-L8	500	240	2.10	1.25	2.08	37.7	0.98	266	317.2	1.19
	S5E-L8	500	240	1.40	1.25	2.08	37.8	0.98	573	596.6	1.04
	S15B-1	1500	240	4.20	3.75	6.25	37.7	0.98	424	424.8	1.00
	S15B-2	1500	240	4.20	3.75	6.25	38.2	0.98	434	428.6	0.99
	S25B-1	2500	240	4.20	6.25	10.42	27.9	0.98	525	502.4	0.96
	S25B-2	2500	240	4.20	6.25	10.42	29.5	0.98	534	520.4	0.97
	S35A-1	3500	240	2.90	8.75	14.58	41.3	0.98	899	977.5	1.09
	S35A-2	3500	240	2.90	8.75	14.58	29	0.98	707	812.7	1.15
	S35B-1	3500	240	4.20	8.75	14.58	35.9	0.98	775	752.4	0.97
	S35B-2	3500	240	4.20	8.75	14.58	38.2	0.98	702	782.8	1.12
	S35C-1	3500	240	5.40	8.75	14.58	39.6	0.98	820	764.2	0.93
	S35C-2	3500	240	5.40	8.75	14.58	29.5	0.98	656	628.4	0.96
	MS5A-dr	500	240	2.90	1.25	2.08	36.9	0.98	280	226.8	0.81
	MS5A	500	240	2.90	1.25	2.08	41.5	0.98	236	244.7	1.04
	MS5B-dr	500	240	4.20	1.25	2.08	37.7	0.98	159	200.5	1.26
	MS35A-dr	3500	240	2.90	8.75	14.58	38	0.98	1058	934.6	0.88
	MS35A	3500	240	2.90	8.75	14.58	37.3	0.98	1283	925.3	0.72
	MS35B	3500	240	4.20	8.75	14.58	38.2	0.98	746	782.8	1.05
	MP35B	3500	240	4.20	8.75	14.58	39.8	0.98	770	803.7	1.04
	MS35B-ρq	3500	240	4.20	8.75	14.58	32.9	0.98	782	712.1	0.91
	MS35C	3500	240	5.40	8.75	14.58	37.3	0.98	741	734.0	0.99
	MS35C-ρq	3500	240	5.40	8.75	14.58	34.9	0.98	657	702.1	1.07
[42]	R0	750	206	4.03	7.50	3.64	29.2	2.2	244	178.4	0.73
	A0	750	206	4.03	7.50	3.64	24.5	2.2	187	161.6	0.86
	C0	750	206	4.03	7.50	3.64	25.2	2.2	182	164.1	0.90
	D0	750	206	4.03	7.50	3.64	32.6	2.2	218	190.1	0.87
[43]	P2	503	142	3.45	8.38	3.54	13.4	0.95	76	57.3	0.75
	P3	502	142	3.45	8.37	3.54	13.4	1.11	81	59.0	0.73
	P8	502	148	3.31	8.37	3.39	24.9	0.91	88	84.1	0.96
	P9	500	146	3.36	8.33	3.42	24.9	1.86	106	94.5	0.89
	P10	503	102	3.43	8.38	4.93	12.4	1.1	59	44.6	0.76
	P12	501	142	2.46	8.35	3.53	12.6	0.95	101	76.9	0.76
[44]	11	1000	500	3.65	10.00	2.00	24.6	0.46	267	303.2	1.14
	16	1000	750	3.67	10.00	1.33	30.4	0.42	407	446.7	1.10
	2	1000	250	3.68	10.00	4.00	26.9	0.64	218	205.3	0.94
	12	1000	500	3.65	10.00	2.00	27.3	0.65	330	342.0	1.04
	3	1000	250	3.68	10.00	4.00	27.3	0.91	223	218.7	0.98
	8	1000	500	5.50	10.00	2.00	31.1	0.63	287	313.7	1.09
	9	1000	500	5.50	10.00	2.00	19.9	0.63	261	241.8	0.93
	10	1000	500	5.50	10.00	2.00	20	0.63	262	242.5	0.93
	17	1000	750	3.67	10.00	1.33	28.7	0.42	364	434.1	1.19
[45]	Real bridge	1000	257	4.38	10.00	3.89	56	1.54	330	345.0	1.05
	lab1	1000	257	2.00	10.00	3.89	60	1.54	620	725.1	1.17
	lab2	1000	257	1.00	10.00	3.89	60	1.54	1000	1290.9	1.29

[46]	64–8F	639	83	4.00	7.70	7.70	30.4	1.88	71	86.2	1.21
	64–8C	640	82	4.00	7.80	7.80	28.5	1.9	85	82.0	0.96
	64–8D	640	81	4.00	7.90	7.90	28.5	1.95	82	81.5	0.99
	48–8B	505	82	4.00	6.16	6.16	27.8	1.98	65	68.6	1.05
	64–8A	640	82	4.00	7.80	7.80	28.5	1.9	87	82.0	0.94
	64–8B	636	81	4.00	7.85	7.85	29.2	1.94	86	82.4	0.96
	64–8F	639	83	4.00	7.70	7.70	30.4	1.88	71	86.2	1.21
	64–8C	640	82	4.00	7.80	7.80	28.5	1.9	85	82.0	0.96
	64–8D	640	81	4.00	7.90	7.90	28.5	1.95	82	81.5	0.99
	48–8B	505	82	4.00	6.16	6.16	27.8	1.98	65	68.6	1.05
	64–8A	640	82	4.00	7.80	7.80	28.5	1.9	87	82.0	0.94
	64–8B	636	81	4.00	7.85	7.85	29.2	1.94	86	82.4	0.96
[47]	N8	500	226	3.50	5.00	2.21	25.8	0.79	102	116.6	1.14
	N6	500	226	2.50	5.00	2.21	25.8	0.79	118	153.1	1.30
	N7	500	225	2.50	5.00	2.22	24.6	1.39	140	185.9	1.33
[48-50]	A1V1	800	156	4.10	8.00	5.13	52.4	1.538	169	212.2	1.26
	A3V1	800	162	3.95	8.00	4.94	58.8	1.745	266	240.6	0.90
	A5V1	800	174	3.68	8.00	4.60	56.7	1.056	222	233.6	1.05
	B1V1	2000	390	4.10	20.00	5.13	52.4	1.538	852	759.0	0.89
	B4V1	2000	420	3.81	20.00	4.76	54.2	0.952	804	778.3	0.97
[51, 52]	VK1V1	2400	224	3.79	6.00	10.71	35	0.81	690	543.0	0.79
	VK2V1	2400	217	3.92	6.00	11.06	46	1.16	678	664.1	0.98
	VK3V1	2400	193	4.40	6.00	12.44	46.5	1.16	672	607.9	0.90
	VK3V3	2400	174	4.89	6.00	13.79	51.5	0.52	644	563.6	0.88
	VK4V1	2400	167	5.09	6.00	14.37	42.5	1.2	487	518.3	1.06
	VK4V3	2400	167	5.09	6.00	14.37	46	0.68	670	519.6	0.78